MOLECULAR ORDER AND DYNAMICS OF 5CB LIQUID CRYSTALS IN CONFINED SPACE – COMPUTER SIMULATION

W. GWIZDAŁA[1] AND Z. GBURSKI[2]

[1] *Pedagogical University*
Chair of Computer Science and Computational Methods
Podchorazych 2, 30-084 Krakow, Poland

[2] *University of Silesia, Institute of Physics*
Uniwersytecka 4, 40-007 Katowice, Poland

(received: 5 December 2014; revised: 12 January 2015;
accepted: 19 January 2015; published online: 16 February 2015)

Abstract: We studied the dynamical and structural properties of an important nematic 4-*n*-pentyl-4'-cyanobiphenyl (5CB) mesogen placed near carbon allotropes (graphene, nanotube), using modeling and molecular dynamics simulations (MD). Every investigated nanosystem (a free cluster of 5CB, a 5CB cluster confined in a single-walled carbon nanotube, 5CB mesogens located between two graphene sheets, a 5CB thin layer on a single-walled carbon nanotube, a thin layer of a 5CB molecules near graphene plane) contains a liquid crystal cluster consisting of 5CB molecules (22–98 molecules). We also performed a computer experiment for a 5CB bulk sample (196 5CB mesogens) with periodic boundary conditions. The following observables were calculated for several temperatures: mean square displacement, radial distribution function and second rank order parameter of 5CB clusters. The obtained results from MD simulations were discussed and compared with the experimental data.

Keywords: liquid crystal, 5CB, carbon nanostructure, nanotube, graphene, computer simulation, MD, second rank order parameter

1. Introduction

This review concerns the physical properties of nematic liquid crystals placed in an unusual environment which includes some of such carbon allotropes as graphene and a carbon nanotube. Despite the fact that liquid crystals have been known and used in the industry for many years, one can still see new papers coming from various research centers around the world. We performed series of computer experiments to explore new structural and dynamic properties of the 4-*n*-pentyl-4'-cyanobiphenyl (5CB) chemical compound. All the physical systems were modeled and numerical calculations were performed using the computer

simulation method. This work consists of two main parts. Its primary aim is to investigate the physical properties of small clusters of mesogen 5CB molecules located near the aforementioned carbon nanostructures. In the first part, one can find essential knowledge about the examined compounds and an introduction to computer simulation techniques. The second part of this work is based on our own research. The last chapter of this paper is analysis and discussion of the results obtained from computer simulations of 5CB mesogens:

- located on the carbon nanostructure surface;
- confined inside a carbon nanotube and between graphene walls.

The motivation to undertake such research topic is the urgent need to gain detailed knowledge about molecular dynamics of mesogens in such specific confined spaces. Particularly, in a perspective of the expected applications in a new generation of future optical devices.

1.1. Liquid crystals: definition, main types and basic properties

1.1.1. Definition of liquid crystals and history note

It is well known that matter can exist in four states: solid, liquid, gas and plasma. However, there are also some mesophases that exhibit properties typical for several other physical states [1]. Molecules in solids are constrained to occupy only certain positions, *i.e.* they have a positional order. Furthermore, molecules in these specific positions are also constrained in the way that they orient themselves with respect to each other, *i.e.* they have an orientational order [2]. The solid may be either crystalline or amorphous. Molecules in liquids move and orient randomly, *i.e.* they lose their positional and orientational order. Molecules in gases also move and orient randomly. The gas and liquid states are very similar with certain differences: while molecules keep an average distance to each other in the liquid state, the average intermolecular distance is determined by the size of the container and the number of molecules in the gas state. The flow is the most important property which differentiates solids and liquids. Liquids flow and adopt the shape of the container, whereas solids do not flow and tend to retain their shape.

In 1888 an Austrian botanist, Reinitzer observed an unusual sequence of phase transition. He observed two melting points while investigating some esters of cholesterol. At 145.5 °C cholesteryl benzoate melted from solid to a cloudy liquid and at 178.5 °C it turned into a clear liquid [2]. In particular, certain organic materials do not show a single transition from solid to liquid, but rather a cascade of transitions involving new phases. The mechanical and symmetry properties of these phases are intermediate between those of a liquid and a crystal. For this reason, they have often been called liquid crystals [1]. Molecules in liquid crystals move randomly like those in a liquid, *i.e.* they have no positional order, but they have some orientational order. A substance is isotropic when its physical properties are the same in all directions; like water at room temperature. Liquid

crystals are anisotropic substances [3] because they exhibit different physical properties in different directions.

Although liquid crystals were discovered as an interesting phenomenon at the end of the 19^{th} century, it took over 30 years of research to establish their true identity. In 1920 Georges Friedel was responsible for recognizing that liquid crystals were indeed a new state of matter that was intermediate in structure and molecular organization between the amorphous liquid state and the solid crystalline state [3].

To better understand the significance of these new states of matters, it may be useful to recall first the difference between a crystal and a liquid. The components of a crystal (molecules, or groups of molecules) are regularly stacked. The mass centers of the various groups are placed in a three-dimensional periodic lattice. The centers of mass are not ordered in this sense in the liquid. These two states of matter differ most obviously by their mechanical properties; a liquid flows easily. A crystal is defined by the fact, that a certain pattern, starting at point x_0, is repeated at $x = x_0 + n_1a_1 + n_2a_2 + n_3a_3$ ($n_i =$ integer; $i \in \{1,2,3\}$ and $\{a_i\}$ basis vectors) stays finite when $|x - x_0| \to \infty$. As a result, its X-ray diffraction pattern shows sharp Brag reflections characteristic of the lattice. An isotropic liquid may be defined in a similar way. One can say that, if one has been able to locate a molecule or some pattern at a given point x_0, there is simply no way to express the probability of finding a similar one at the point x far from x_0, except through the average particle density [1].

We are now able to give the definition of liquid crystals. These are systems in which a liquid-like order exists at least in one direction of space and in which some degree of anisotropy is present (a better definition of "some degree of anisotropy" is: the density-density correlation function does not depend solely on modulus $|x - x'|$ but also on the orientation of $x - x'$ with respect to the macroscopically defined axes) [1].

1.1.2. General types and liquid crystal phases

Considering the geometrical structure of the mesogenic molecules, the liquid crystals can be grouped into several types. Mesophases formed from disc-like molecules (one molecular axis is much shorter than the other two) are referred to as "discotics" (Figure 1a). Liquid crystals derived from rod-shaped molecules (one axis is much longer than the other two) are called "calamitics" (shown in Figure 1b). This class of materials is well known and extremely useful for practical applications [2]. Transitions to mesophases may be brought about in two different ways; one by ordinary thermal processes and the other by the influence of solvents. Liquid crystals obtained by the former method are called "thermotropics" whereas those obtained by the latter method are "lyotropics". This work focuses on the dynamical and structural properties of "thermotropic" rod-like mesogens.

As far as we know there are several liquid crystalline phases. The simplest one that could be imagined is a phase in which the molecules are oriented along

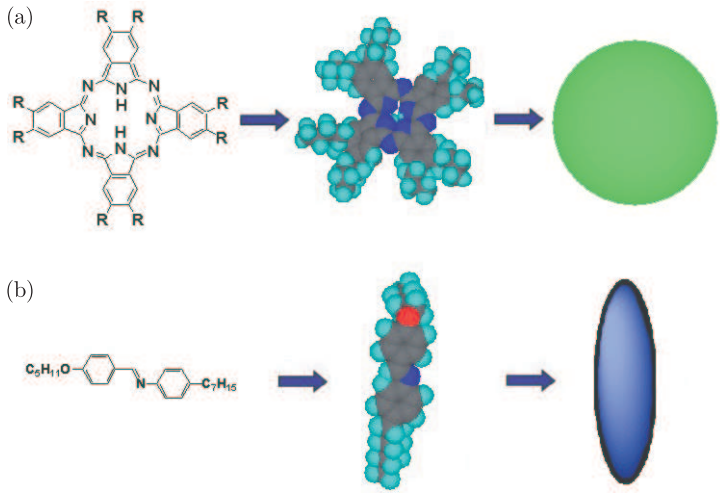

Figure 1. (a) Phthalocyanine and disc-shape; (b) 4-*n*-heptyl-*N*-(4-*n*-pentyloxy) benzylideneand rod-shape

a common direction in space, and the positions of molecules are totally random [4]. In other words, molecules have no positional order but they self-align to have a long-range directional order with their long axes roughly parallel. A schematic picture of this phase is shown in Figure 2.

Figure 2. Nematic phase represented schematically

Molecules appear to be able to rotate along their long axes and also there seems to be no preferential arrangement of the two ends of molecules, if they differ. This phase is an oriented or anisotropic liquid. Such liquids are frequently observed in nature and are called nematic liquid crystals. Many compounds are known to form a nematic mesophase. A few typical examples are sketched in Figure 3.

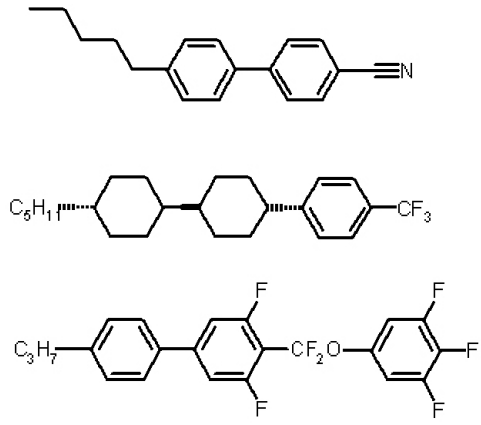

Figure 3. Nematic molecules; rigid rod ~ 20 Å long and ~ 5 Å wide

The cholesteric phase looks like the nematic phase in having a long-range orientation order and no long-range order in positions of the centers of mass of molecules (Figure 4). This distortion has been first observed in liquid crystals which contain cholesterol, thus, for historical reasons, this structure, which is a unique phase, is called the cholesteric liquid crystalline phase. There are many liquid crystals which exhibit a cholesteric phase but have no connection to cholesterol. For this reason, a much better name to use is a chiral nematic or a twisted nematic. Locally, a cholesteric phase seems to be like a nematic. When the structure is studied over large enough distances it seems that the cholesteric phase appears to have a structure different from the nematic phase [4].

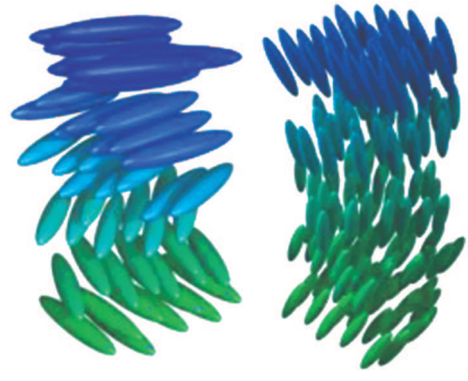

Figure 4. Cholesteric phase

Suppose now that a phase form in which the long-range orientational order is maintained and long-range periodicity is found, not in three dimensions as in a crystal, but only in one dimension. This can be considered as a stack of two-dimensional liquid surfaces. The spacing between these liquid surfaces extends

over very long distances resulting in a phase with a long-range orientational order and a long-range positional order in one dimension. This type of a liquid crystalline phase exists also in nature and is known as a smectic liquid crystal. The molecules are arranged in layers and show some correlations in their positions in addition to the orientational ordering. Different types of smectics have been recognized and classified. In the smectic A phase the molecules are aligned perpendicular to the layers, with no long-range crystalline order within a layer (see Figure 5). In the smectic C phase, the preferred axis is not perpendicular to the layers, thus the phase has biaxial symmetry. A hexagonal crystalline order within the layers is visible in the smectic B phase.

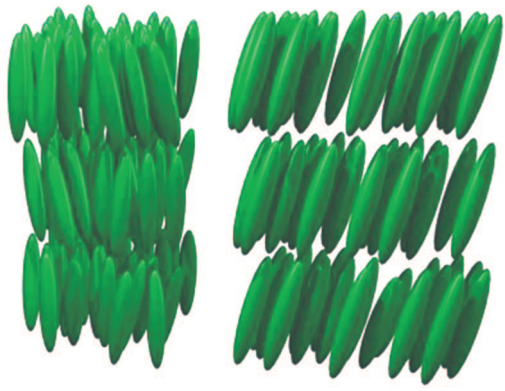

Figure 5. Smectic A representation (left); Smectic C representation (right)

Another most complex phase would be a phase that has a long-range orientational order and a long-range positional order in two dimensions. Such a phase can be described as a two-dimensional array of liquid tubes. Such phases are also observed and are called columnar phases.

All listed and discussed phases (nematic, smectic and columnar) are the only known liquid crystalline phases. However, slight variations in these basic phases occur and lead to hyphenated names for some existing phases. The type of phase observed depends very strongly on the structure of the constituent molecules or, in some situations, the aggregates that constitute the phase. Nematics and smectics are most often observed for elongated or rod-like molecules. Columnar phases are often observed for disc-like molecules [4, 5].

1.1.3. Physical properties of liquid crystals

Liquid crystalline materials are anisotropic because they are composed of anisotropic molecules. Some of their physical properties depend on the direction along which they are measured. Such properties are known as tensor properties. A comfortable way of categorizing tensor properties is through their behavior on changing the orientation of a coordinate system. A scalar or zero rank tensor is independent of direction. Good examples are density, volume, energy or any

orientationally averaged property such as the mean polarizabilty or mean electric permittivity (dielectric constant). The orientation dependence of a vector property such as dipole moment μ can be explained by considering how the components of the dipole moment change as the coordinate system axis are rotated [6].

The liquid crystalline materials exhibit anisotropy in many of their physical properties. Due to these anisotropies and their resulting interactions with the surrounding environments a number of phenomena are found in a liquid crystalline phase which are absent in the isotropic liquid phase. A brief discussion on some of these properties is given in the following.

It is well known that liquid crystals are sensitive to an electric field. This fact enables their application in displays and other optical devices. The optical anisotropy is an essential physical property for the optimization of liquid crystal compounds for application in liquid crystal devices. The velocity of light wave propagation in the medium is no longer uniform but is dependent upon the direction and polarization of the light waves transversing the material; thus the material is found to possess different refractive indices in different directions. Aligned liquid crystals allow controlling the polarization of light which has resulted in the use of liquid crystals in displays [2]. The ordinary refractive index n_0 can be observed with a light wave where the electric vector oscillates perpendicular to the optic axis. The extraordinary refractive index n_e is observed for a linearly polarized light wave where the electric vector is vibrating parallel to the optic axis. The optic axis of the uniaxial mesophases is represented by the director. The optical anisotropy, or birefringence is wave length and temperature dependent and defined by the equation:

$$\Delta n = n_e - n_0 = n_{\parallel} - n_{\perp} \tag{1}$$

where $n_{\parallel}$ and $n_{\perp}$ are the components parallel and perpendicular to the director, respectively [2].

Polarizability: An electric field can polarize atoms and molecules. The polarization (induced dipole of a unit volume) can be defined as $\vec{P} = \alpha \vec{E}$, where α is molecular polarizability and $\vec{E}$ is the electric field intensity. For spherically symmetric objects, atoms or molecules (like C_{60} fullerenes), the polarizablity is a scalar quantity (tensor of zero rank) and $\vec{P} \parallel \vec{E}$. In a general case of lath-like molecules, α_{ij} is a second rank tensor (consisting of 9 components) and $\vec{P}_j = \alpha_{ij}\vec{E}_i$ by a proper choice of the reference frame the tensor can be diagonalized

$$\alpha_{ij} = \begin{bmatrix} \alpha_{xx} & 0 & 0 \\ 0 & \alpha_{yy} & 0 \\ 0 & 0 & \alpha_{zz} \end{bmatrix} \tag{2}$$

and components α_{xx}, α_{yy} and α_{zz} represent three principal molecular polarizabilities. For molecules which have cylindrical symmetry (rods or disks) with the symmetry axis z, only two different components remain $\alpha_{xx} = \alpha_{yy} = \alpha_{\perp}$ and $\alpha_{zz} = \alpha_{\parallel}$.

Permanent dipole moments: If a molecule has an inversion centre it is non-polar and its dipole moment $\vec{p}_e = 0$. The dipole moment is finite in less symmetric cases. This observable is measured in Debye units and in the Gauss system $1\,\mathrm{D} = 10^{-18}\,\mathrm{CGSQ{\cdot}cm}$ ($3.3 \cdot 10^{-30}\,\mathrm{C{\cdot}m}$ in SI system). In other words, 1 D corresponds to one electron positive and one electron negative charge separated by a distance of $\approx 0.2\,\text{Å}$. For a complex molecule can be estimated as a vector sum of the moments of all intramolecular chemical bonds, $\vec{p}_e = \sum \vec{p}_i$. A classical example is shown in (Figure 6). A molecule of 5CB (4-*n*-pentyl-4'-cyanobiphenyl) investigated in this work has a longitudinal electric dipole moment about 3D due to a triple $-\mathrm{C}{\equiv}\mathrm{N}$ bond.

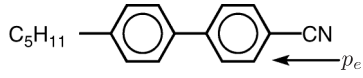

Figure 6. 5CB mesogen molecule

The vector of a permanent dipole moment and polarizability tensor is used to describe the linear (in field) electrical and optical properties. The nonlinear properties are described by tensors of higher ranks.

Magnetic moments: A magnetic field induces magnetic moments in a molecule and is given by the relation: $p_{mi} = m_{ik} \cdot H_k$, where m_{ik} is the diamagnetic susceptibility tensor. It has the same structure as the tensor of molecular polarizability with three or two different principal components. Some molecules possess permanent magnetic moments. For example, the moments originate from unpaired electron spins in the inner shells of such metal atoms as $M = \mathrm{Ni}$, Co, Fe, *etc.* in metal-mesogenic compounds. In other cases it depends on free radicals with permanent magnetic moments such as -NO molecular groups, in which unpaired electron spins are placed on oxygen atoms. The stability of such radicals is provided by sterical screening of a reaction centre from the surrounding medium by bulky chemical groups (like the methyl one). Such a radical can be a fragment of a longitudinal mesogenic molecule. It is important that the field orientation of spin moments is almost decoupled from the molecular skeleton motion (in contrast to electric moments of molecular groups). It should be noted that the simultaneous orientation of spins and molecular skeletons by a magnetic field takes place only if the spin-orbital interaction is significant [7].

1.1.4. Molecular ordering

In the crystalline (solid) state, molecules usually have a near-perfect orientational order. In the mesophase this degree of order is partially but not completely lost, as the molecules show highly dynamic behavior and only one average point in the same direction. This preferred direction is called the director (Figure 7). The most common liquid crystalline phase (nematic) has a lower symmetry than the high-temperature isotropic liquid, hence it means that the nematic phase is "more ordered". The degree of order is described by the order parameter (P), which is a measure for the average angle θ between the director and the long axes

of the mesogens. It is essential to define an order parameter that is non-zero in the nematic phase but that vanishes in the isotropic phase. For an isotropic sample, $P=0$, whereas for a perfectly aligned crystal $P=1$. For a typical liquid crystal, P is between 0.3 to 0.8, and this value generally decreases due to higher mobility and disorder as the temperature is raised (thermotropic mesogens). In some physical ensembles an adequate choice of the order parameter is obvious. For instance, in a ferromagnet, the magnetization M is the order parameter and in a such case this is a vector with three independent components M_Φ. In a nematic phase the choice is less trivial and we have to proceed in successive steps [1].

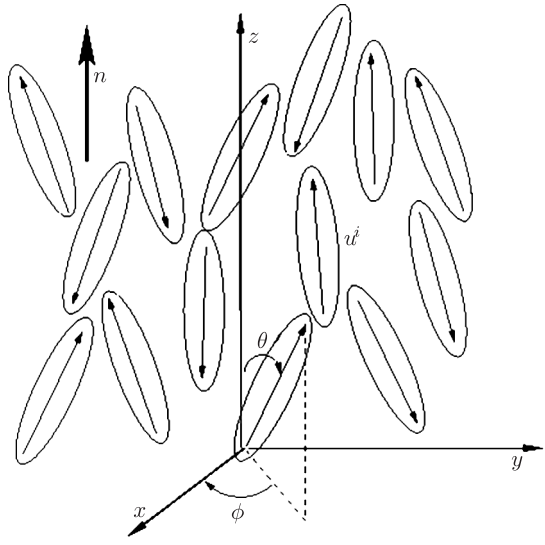

Figure 7. A unit vector u^i along the axis of i^{th} molecule describes its orientation. The director n shows the average alignment

If the laboratory Z axis is taken parallel to the director and if the mesophase is uniaxial around the director then rotating the sample about Z should leave all the observable properties unchanged. This means that the probability for a molecule to have an orientation (Φ,θ) is the same for all values of the rotation angle [8]. More precisely

$$P(\Phi,\theta)=\frac{P(\theta)}{2\pi} \tag{3}$$

Another experimental finding for nematics is that no physical properties change if the aligned sample is turned upside down:

$$P(\theta)=P(\pi-\theta) \tag{4}$$

This is quite reasonable if we consider the molecules of interest as spherocylinders or other cylindrically symmetric objects in which head and tail are not distinguishable. However, most mesogens do not possess such properties and for instance have permanent dipole moments like p-n alkyl p'-cyano biphenyls (nCB). In practice the symmetry represented in Equation (4) means that the molecular

arrangement will be such to have no overall sample polarization (no ferroelectricity) as we show schematically in Figure 8. It is impossible to give fundamental argument that would forbid uniaxial ferroelectric fluids and indeed these have been predicted by theory and simulations [9], although they have not been experimentally found yet. It should be noticed that the same notation for $P(\theta)$ and $P(\cos\theta)$ has been used, that we assume to be renormalized to 1.

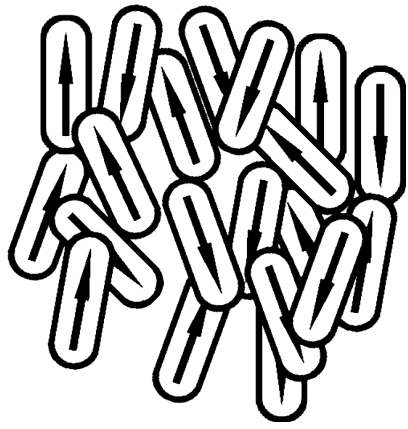

Figure 8. Schematic molecular organization for a system of polar molecules with no overall polarization

In a real experiment it could be extremely difficult to obtain this kind of complete information on the orientational distribution. However, a useful approach is that of expanding $P(\theta)$ and approximating it in terms of a set of quantities that could be obtained from experiment. A set of functions (orthogonal) is necessary when integrated over $d\theta\sin\theta$ Such a set of functions is that of Legendre polynomials $P_L(\cos\theta)$, for which the following formula is given

$$\int_0^\pi d\theta\sin\theta P_L(\cos\theta)P_N(\cos\theta) = \frac{2}{2L+1}\delta_{LN} \tag{5}$$

The explicit form of these Legendre polynomials is not very complex [10] and the first few terms are:

$$P_0(\cos\theta) = 1 \tag{6}$$

$$P_1(\cos\theta) = \cos\theta \tag{7}$$

$$P_2(\cos\theta) = \frac{3}{2}\cos^2\theta - \frac{1}{2} \tag{8}$$

$$P_3(\cos\theta) = \frac{5}{2}\cos^3\theta - \frac{3}{2}\cos\theta \tag{9}$$

$$P_4(\cos\theta) = \frac{35}{8}\cos^4\theta - \frac{30}{8}\cos^2\theta + \frac{3}{8} \tag{10}$$

It is worth noting that $P_L(\cos\theta)$ is an even function of $\cos\theta$ if the rank L is even and an odd one if L is odd. Since $\cos(\Pi-\theta) = -\cos\theta$, it is only the terms with even L that need to be kept in even orientational distributions written in

terms of the $P_L(\cos\theta)$ functions. Clearly the odd terms will be exhibited if $P(\theta)$ is not even, as for ferroelectric liquid crystalline phases. Limiting ourselves to the more common even (see Equation (4)) case it can be given as:

$$P(\theta) = \sum_{L=0}^{\infty} \frac{2L+1}{2} \langle P_L \rangle P_L(\cos\theta) \text{ for } L = 0,2,4,\ldots \tag{11}$$

where the coefficients have been obtained exploiting the orthogonality of the basis set. The average values of $\langle P_L \rangle$:

$$\langle P_L \rangle = \frac{\int_0^{\pi} d\theta \sin\theta P_L(\cos\theta) P(\theta)}{\int_0^{\pi} d\theta \sin\theta P(\theta)} \tag{12}$$

represent a set of orientational order parameters. The knowledge of the set of $\langle P_L \rangle$, which is infinite, would completely define the distribution. The next formula arises from Equation (11):

$$P(\theta) = \frac{1}{2} + \frac{5}{2} \langle P_2 \rangle P_2(\cos\theta) + \frac{9}{2} \langle P_4 \rangle P_4(\cos\theta) + \ldots \tag{13}$$

The first term contains the second rank order parameter:

$$\langle P_2 \rangle = \frac{3}{2} \langle \cos^2\theta \rangle - \frac{1}{2} \tag{14}$$

It is really easy to see that $\langle P_2 \rangle$ has the properties an order parameter is expected to possess and that can be identified with the empirical parameter which was introduced by Tsvetkov [11]. For a system of perfectly aligned mesogenic molecules, where $\theta = 0$ for every molecule, $\langle P_2 \rangle = 1$. At the other extreme, for a completely disordered sample such as an ordinary isotropic fluid $\langle \cos^2\theta \rangle = 1/3$ and thus $\langle P_2 \rangle = 0$. In a general case:

$$-\frac{1}{2} \leq \langle P_2 \rangle \leq 1 \tag{15}$$

because $0 \leq cos^2\theta \leq 1$. During transition from an ordered to a disordered system the order parameter jumps discontinuously to zero, if the transition is of the first order type, like the nematic-isotropic one. It is worth knowing that the same $\langle P_2 \rangle$ can correspond to different molecular organizations [12, 13].

1.2. Forms of Carbon: Diamond, Nanotubes, Graphite and Graphene

1.2.1. The carbon atom chemistry

Carbon is essential to all the known living systems, and without it life as we know it could not exist. A carbon atom is placed directly above silicon on the periodic table and therefore both have 4 valence electrons. These valence electrons give rise to $2s$, $2px$, $2py$, and $2pz$ orbitals while the 2 inner shell electrons belong to a spherically symmetric $1s$ orbital that is tightly bound. For this reason, it is only the electrons in the $2s$ and $2p$ orbitals that contribute to the solid-state properties of graphite. The extraordinary ability to hybridize sets carbon apart

from other elements and allows carbon to form 0D, 1D, 2D, and 3D structures (Figure 9) [14].

The applications of carbon and its compounds are extremely varied. It can form alloys with iron, of which the most common is carbon steel. Graphite is combined with clays to form the "lead" used in pencils. It is also used as a lubricant and a pigment, as a molding material in glass manufacture, in electrodes for dry batteries, in brushes for electric motors and as a neutron moderator in nuclear reactors.

1.2.2. Carbon allotropes

Diamond: The diamond is a three dimensional form of carbon. It poses *sp*3 hybridization, forming 4 covalent bonds with the neighboring carbon atoms into a face-centered cubic atomic structure. As the carbon-carbon covalent bond is known as one of the strongest in nature, diamond has a remarkably high Young's modulus and high thermal conductivity. An undoped (pure) diamond has no free electrons and is a wide band gap ($\sim 5.5\,\mathrm{eV}$) insulator [15]. The exceptional physical properties and clever advertising such as "Diamonds are forever" contribute to its appeal as a sought after gem. It can be used to make beautiful pieces of jewelry, but only when carefully cut and polished. Crystals with smaller defects are used as reinforcement in tool bits which utilize their superior hardness for cutting applications. The high thermal conductivity of diamond makes it a potentially useful material for microelectronics where the problem of heat dissipation is a serious issue. However, as diamonds are scarce they are unappealing. To this end, scientists and engineers are focused on trying to grow large diamond wafers. One method to do this is chemical vapor deposition (CVD) where solid carbon is deposited from carbon containing such gases as methane or ethylene. By controlling the growth conditions, it is possible to produce high quality diamonds (without defects) of limited size. This technique is widely used to produce diamonds for jewelry and research is ongoing to scale the technology up to the wafer size diamond growth. It is only with such large scale growth that the diamond will make any technological impact beyond its current industrial uses in the machining industry.

Fullerenes: Carbon exists also in more exotic low dimensional forms known as fullerenes which consist of the 0 dimensional C60 molecule (Figure 9b) and its 1 dimensional derivative, carbon nanotubes. A single-walled carbon nanotube (SWCNT) is a graphene sheet rolled into a cylindrical tube with a $\sim 1\,\mathrm{nm}$ diameter (Figure 9a). The first reported observation of carbon nanotubes was by Iijima in 1991 for multi-wall nanotubes (MWNT) [16]. Two years later, single-walled carbon nanotubes were discovered experimentally by Iijima [17] at the NEC Research Laboratory in Japan and by Bethune [18] at the IBM Almaden Laboratory in California. These experimental discoveries and the theoretical works which predicted many remarkable and interesting properties for carbon nanotubes, launched this field and propelled it forward. Carbon nanotubes can be both metals or semiconductors and have mechanical strength similar to the

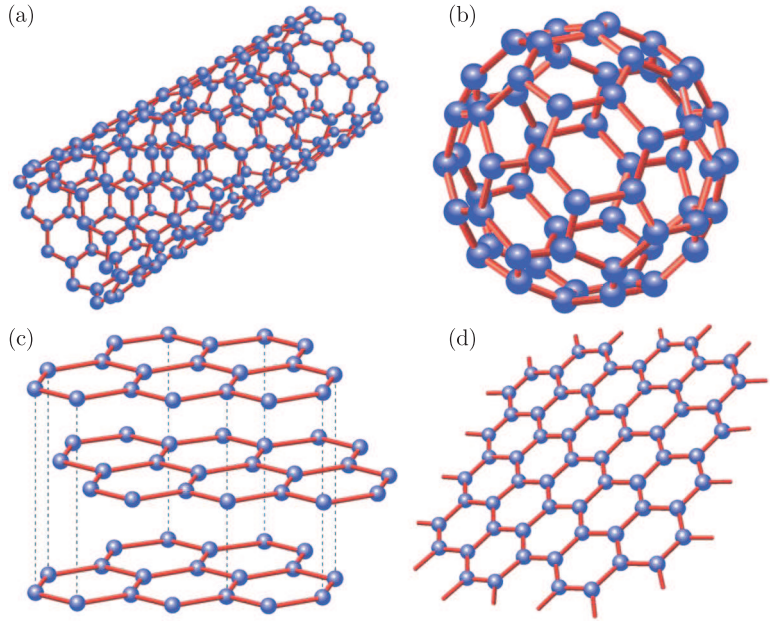

Figure 9. (a) Single-walled carbon nanotube; (b) Buckminsterfullerene (C_{60}); (c) Graphite lattice; (d) Graphene sheet

diamond. These carbon allotropes attracted a lot of attention from the research community and dominated the scientific headlines during the 1990s and the early 2000s. This interest in carbon nanotubes was partly responsible for the search for planar two-dimensional carbon structures as a potentially important and interesting material for electrical and mechanical applications [19–21].

Graphite and Graphene: Graphene and graphite are the two-dimensional *sp2* hybridized forms of carbon, used in the pencil lead. Graphite is a layered material formed by stacks of graphene planes separated by 0.335 nm and held together by weak van der Waals forces (Figure 9c) [22]. This type of interaction between the sheets allows them to slide relatively easily across one another. This gives pencils their writing ability and graphite its lubricating properties, however, the nature of this interaction between layers is not quite understood. It has been well known for decades that the presence of water reduces the frictional force considerably [23]. Another frictional effect is the registry of a lattice between the layers. Mismatch in this registry is believed to give graphite the property of superlubricity where the frictional force is reduced distinctly [24]. Zheng [25] claims that mechanical experiments based on few-layer graphene may help to elucidate some of these mechanisms clearly. A single 2D surface of graphene is a hexagonal structure with each atom forming 3 bonds with each of its nearest neighbors (Figure 10d). These are the σ bonds oriented towards these neighboring atoms and formed from 3 of the valence electrons. These covalent carbon-carbon bonds are nearly the same as the bonds holding diamond together giving graphene similar mechanical and thermal properties as

diamond. The fourth valence electron does not participate in covalent bonding at all. It is in the $2p_z$ state oriented perpendicular to the plane of graphite and forms a conducting π band. The unusual electronic properties of carbon nanotubes are a direct consequence of the peculiar band structure of graphene, a zero bandgap semiconductor with 2 linearly dispersing bands that touch at the corners of the first Brillouin zone [26]. Bulk graphite has been intensively investigated for decades [22] but until recently there were no experiments on graphene. This was due to the difficulty in separating single layers of graphene for study. In 2003, Novoselov and Geim succeeded in producing the first isolated graphene flakes [27].

1.3. Computer simulation: molecular dynamics simulations

1.3.1. Introduction to computer simulations

Before computer simulation appeared as a research technique, there was only one way to predict the properties of a molecular substance, namely by making use of a theory that provided an approximate description of that material. Such approximations are inevitable inaccurate because there are very few systems like for instance the ideal gas, the harmonic crystal, and a number of lattice models, such as the two-dimensional Ising model for ferromagnets for which the equilibrium properties can be computed exactly. Most properties of real materials were predicted on the basis of approximate theories (good examples are the van der Waals equation for dense gases, the Debye-Htickel theory for electrolytes, and the Boltzmann equation to describe the transport properties of dilute gases). Having information about the intermolecular interactions, these theories will provide us with an estimate of the properties of interest. Our knowledge of the intermolecular interactions of all but the simplest molecules is also quite limited. This leads to a problem if we want to test the validity of a particular theory by comparing to experiment. If we find that theory and experiment disagree, it may mean that our theory is wrong, or that the estimate of the intermolecular interactions is incorrect, or both [28]. It is now over 60 years since the first computer simulation of a liquid was performed by Metropolis et al. at the Los Alamos National Laboratories in the United States [29]. MANIAC – the Los Alamos computer was at that time one of the most powerful available computers; it is a measure of the recent rapid advance in computer technology that microcomputers of comparable power are now available to the general public at moderate cost [30]. The two main families of computer simulations are molecular dynamics (MD) and Monte Carlo (MC); additionally, there is a whole range of hybrid techniques which combine features from both.

Early models of liquids involved physical manipulation and analysis of the packing of a large number of gelatin balls, representing molecules; this resulted in a surprisingly good three-dimensional picture of the structure of a liquid and later applications of the technique have been described. Even nowadays, there is some interest in the study of assemblies of metal ball bearings, kept in motion by mechanical vibration. However, the use of large numbers of objects to represent

molecules can be very time-consuming, there are obvious limitations on the types of interactions between them, and the effects of gravity can never be eliminated. The natural extension of this approach is to use a mathematical model and to perform the analysis by computer [30].

From the outset, computers have been playing a central role in scientific research, both in experiment and in theory. For the theoretician physicist, the computer has provided a new paradigm of understanding. Rather than attempting to obtain simplified closed-form expressions that describe behavior by resorting to approximation, the computers are now able to examine the original system directly. Despite the fact that there are no analytic formulas to summarize the results neatly, all aspects of the behavior are open for inspection [31].

1.3.2. Atomic model and interaction potential

The most simple microscopic model for a substance capable of existing in any of the three most familiar states of matter – solid, liquid and gas – is based on spherical particles. They interact with one another; in the interest of brevity such particles will be referred to as atoms. The interactions, at the simplest level, occur between pairs of atoms and are responsible for providing the two principal features of an interatomic force. Resistance to compression is the first feature, hence the interaction repels at close range. The second feature is to bind the atoms together in solid and liquid states, and for this the atoms must attract each other over a range of isolation. Potential functions which exhibit these characteristics can adopt a variety of forms and actually provide useful models for real substances.

The most popular of these potentials, originally proposed for liquid argon, is the Lennard-Jones (LJ) potential V_{LJ} (Figure 11), that depends on two parameters: length-scale parameter , and energy-scale parameter ε. The simplest form of $V_{\mathrm{LJ}}(r)$ is given via the formula:

$$V_{\mathrm{LJ}}(r_{ij}) = 4\varepsilon\left[\left(\frac{\sigma}{r_{ij}}\right)^{12} - \left(\frac{\sigma}{r_{ij}}\right)^{6}\right] \tag{16}$$

for a pair of atoms i and j located at $\vec{r}_i$ and $\vec{r}_j$ respectively, $r_{ij} = |\vec{r}_i - \vec{r}_j|$, $r_{ij} < r_c$, and zero otherwise. If r increases towards r_c (cutoff radius) the potential energy $V(r)$ drops to zero:

$$V(r) = \begin{cases} V_{\mathrm{LJ}}(r), & r \le r_c \\ 0, & r > r_c \end{cases} \tag{17}$$

Ignoring the calculations of all interactions beyond r_c is the simplest method to truncate the potential. This kind of a numerical trick is often used in performing simulations of a systems with short-range interactions. The equations of motion imply from Newton's second law that:

$$m_i\ddot{\vec{r}}_i = \vec{F}_i = \sum_{j=1,(j\neq i)}^{N_m} \vec{F}_{ij} \tag{18}$$

where the sum is over all N_m interacting atoms, excluding i itself, and m is the atomic mass. These equations must be numerically integrated. Newton's third law

shows that $F_{ji} = -F_{ij}$, hence each atom pair needs to be examined only once. The number of interactions is proportional to N_m^2, so that for models in which cutoff distance r_c is small compared with the size of the container it would be a good idea to determine those atom pairs for which $r_{ij} \leq r_c$ and use this information to reduce the computational effort [31].

2. Computer Simulation Model

2.1. Molecular modeling

Molecular modeling techniques encompass all theoretical and computational methods used to describe molecules and are used in the fields of computational chemistry, biology, physics, *etc.* The common feature of these techniques is the atomistic level description of the molecular systems. The lowest level of information is single atoms or a small group of atoms (so-called "superatoms"). This is in contrast to quantum chemistry (electronic structure calculations) where electrons are considered explicitly. Molecular modeling gives a very important benefit as it reduces the complexity of the system, allowing many more objects (particles or atoms) to be considered during simulations. When molecules are near enough to interact, we must concern ourselves with the balance between the forces of attraction and repulsion. It is well known that such forces exist, otherwise there would be nothing to bring molecules together into the solid and liquid states, and all matter would be gaseous. A study of the forces between atomic or molecular species constitutes the issue of intermolecular forces [32]. We know there are two main kinds of a molecule model: a rigid molecule (rigid chemical bonds) and a flexible model (elastic bonds). Calculations in this work have been done using the latter and all details are described in the next subsection.

2.2. Elastic bonds

The study of molecules with elastic bonds has been one of the main areas of interest during the last years [33–37]. For instance such molecules like *n*-butane do not have a rigid permanent shape. In fact they may adopt many different shapes or conformations. For example *n*-butane can exist in the spatial configuration denoted as trans (where all C atoms are in a plane) or in the spatial configuration denoted as gauche (where one of the C atoms is out of the plane). In a liquid sample of a fluid with flexible molecules such as *n*-hexane, some particles adopt the whole trans configuration, other adopt a configuration with all bonds in the trans configuration but one in the gauche configuration *etc.* The spatial molecular shape is dynamic in the sense that a given molecule adopts a number of different spatial configurations in time. Alkanes are a well known and typical example of flexible molecules.

We have chosen the 4-*n*-pentyl-4'-cyanobiphenyl (5CB) molecule as a typical representative of mesogens. This molecule has been studied extensively both theoretically and experimentally and therefore a large data set is available for confrontation with the results from a computer simulation. One reason for this

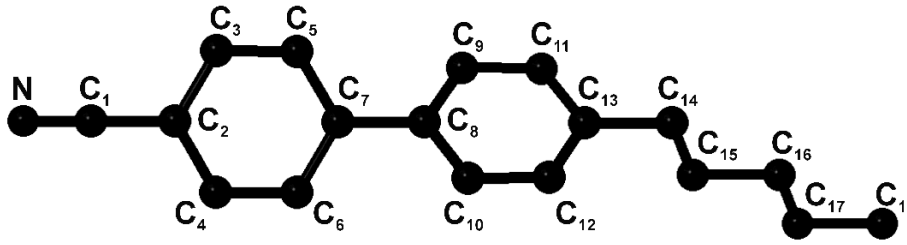

Figure 10. Model of 5CB molecule (without hydrogen atoms)

large number of experimental investigations is the convenient temperature range of the nematic phase, namely, from 295.6 to 308.5 K [34].

The 5CB mesogens (Figure 10) were treated as flexible and modeled by the CHARMM 27 force field [38], which includes intramolecular harmonic stretching, harmonic bending, torsional, van der Waals and Coulombic terms. The form of the potential energy function is given by the following equation:

$$V_{\text{total}} = V_{\text{stretch}} + V_{\text{bend}} + V_{\text{vdW}} + V_{\text{Coulomb}} + V_{\text{torsional}} \tag{19}$$

$$\begin{aligned} V_{\text{total}} = {} & K_r(r-r_0)^2 + K_\Theta(\Theta-\Theta_0)^2 + 4\varepsilon\left[\left(\frac{\sigma}{r}\right)^{12} - \left(\frac{\sigma}{r}\right)^{6}\right] \\ & + \frac{e^2}{4\pi\varepsilon_0 r} + \begin{cases} K_\varphi\big(1+\cos(n\varphi-\gamma)\big), & n \neq 0 \\ K_\varphi(\varphi-\gamma)^2, & n = 0 \end{cases} \end{aligned} \tag{20}$$

The use of full atomistic potential, which includes all hydrogens, is very demanding in terms of computer resources, and it is worth asking if a slightly smaller resolution, such as that afforded by the united-atom (UA) approximation [30], where CH, CH_2 and CH_3 groups are considered as suitably parameterized spherical interaction sites.

Carbon nanostructures (nanotube and graphene) have also been modeled using a flexible model based on the CHARMM 27 force field.

Interactions between CNS and 5CB molecules have been described by usual Lennard-Jones 12–6 potential with Lorentz-Berthelot mixing rules $\sigma_{A-B} = (\sigma_A + \sigma_B)/2$ and $\varepsilon_{A-B} = \sqrt{\varepsilon_A \varepsilon_B}$ [30]. Specifications of the force field parameters

Table 1. Description of atoms forming 5CB mesogenic molecule and carbon nanostructures

Atom type	Site	Description
N	N	*sp* nitrogen
C0	C_1	*sp* carbon without hydrogens
C00	C_2, C_7, C_8, C_{13}	sp^2 carbon without hydrogens
C1	C_3–C_6, C_9–C_{12}	sp^2 carbon with 1 hydrogen
C2	C_{14}–C_{17}	sp^3 carbon with 2 hydrogens
C3	C_{18}	sp^3 carbon with 3 hydrogens
C (CNS)	C	aromatic sp^2 carbon (from carbon nanostructure)

for all interactions are given in Table 2. The charge distribution on 4-*n*-pentyl-4'-cyanobiphenyl mesogen has been calculated on an ab initio level [37] and is presented in Table 3. Similarly to the rigid model, which is described in a previous subsection in detail, there is no electric charge on carbon atoms of CNS (nanotube, graphene).

2.3. Description of calculated observables

The physical properties of 5CB mesogens were studied by calculating several dynamical and structural characteristics. All these observables give us much useful information about the investigated molecular system. The numerical and mathematical procedures are described in two subsections (2.3.1 and 2.3.2). All algorithms for basic data analysis from molecular dynamics trajectories were implemented in the C++ programming language.

2.3.1. Dynamical properties

Dynamical observables are used to investigate physical properties of samples. Numerical methods with visualization allow us to better understand and explain the basic properties.

We know that there are two types of velocity of a molecule: linear $\vec{v}$ and angular $\vec{\omega}$. To obtain physically meaningful information basing on these observables, it is convenient to calculate the velocity autocorrelation function (VACF):

$$C_v(t) = \frac{\langle \vec{v}(t) \cdot \vec{v}(0) \rangle}{\langle \vec{v}(0)^2 \rangle} \tag{21}$$

$$C_\omega(t) = \frac{\langle \vec{\omega}(t) \cdot \vec{\omega}(0) \rangle}{\langle \vec{\omega}(0)^2 \rangle} \tag{22}$$

where $\langle \ldots \rangle$ represents average over time and molecules in the ensemble.

These functions are of great interest in a computer simulation due to the following reasons:

(1) they give a very clear picture of the dynamics in fluids;
(2) their time integrals may almost always be related directly to the macroscopic transport coefficient;
(3) their Fourier transforms may usually be related to experimental spectra [30].

The thermal motion of molecules in the liquid or gas phase is often described as a diffusion process. Diffusion of a labeled species among otherwise identical molecules is called self-diffusion. The translational diffusion coefficient D shows how fast that phenomena occurs and is directly connected with the mean square displacement $\langle |\Delta r(t)|^2 \rangle = \langle |\vec{r}(t) - \vec{r}(0)|^2 \rangle$.

D is a macroscopic transport coefficient and $\langle \vec{r}^2(t) \rangle$ has microscopic interpretation: it is the mean-squared distance over which the labeled molecules have moved in a time interval t.

Table 2. CHARMM force field parameters for 5CB (taken from [37], see supporting information) and carbon nanostructures

Stretching type			
$V_{\text{stretch}} = K_r(r - r_0)^2$	K_r [kcal mol^{-1}Å^{-2}]	r_0 [Å]	
C00–C0	95.9	1.42	
C1–C1	469.0	1.41	
C00–C1	469.0	1.41	
C00-C00	469.0	1.48	
C2–C2	95.9	1.54	
C2–C3	95.9	1.54	
C0–N	600.0	1.16	
C00–C2	317.0	1.51	
C–C (CNS)	305.0	1.38	
Bending type			
$V_{\text{bend}} = K_\Theta(\Theta - \Theta_0)^2$	K_Θ [kcal mol^{-1}rad^{-2}]	Θ_0 [degrees]	
C2–C2–C2	63.0	112.4	
C2–C2–C3	62.1	114.0	
C3–C2–C3	62.1	114.0	
C00–C00–C1	85.0	120.0	
C1–C00–C1	85.0	120.0	
C00–C1–C1	85.0	120.0	
CY–C00–C1	85.0	120.0	
C00–C0–N	79.5	180.0	
C1–C00–C2	70.0	120.0	
C00–C2–C2	63.0	112.4	
C–C–C (CNS)	40.0	120.0	
Torsion type			
$V_{\text{torsional}} = \begin{cases} K_\varphi(1+\cos(n\varphi-\gamma)), & n \neq 0 \\ K_\varphi(\varphi-\gamma)^2, & n = 0 \end{cases}$	K_Φ [kcal mol^{-1}]	n	γ [degrees]
C00–C1	2.65	2	180
C1–C1	5.3	2	180
C2–C00	0.5	6	0
N–C0–C00–C1	0.0	1	180
C2–C2	0.6706	1	0
C2–C2	0.1365	2	0
C2–C2	1.4	3	0
C00–C00	0.010	1	180
C00–C00	0.692	2	180
C00–C00	0.001	3	180
C00–C00	1.064	4	0
C–C–C–C (CNS)	3.1	2	180

Table 2 – continued. CHARMM force field parameters for 5CB...

van der Waals type			
$V_{\mathrm{vdW}} = 4\varepsilon\left[(\sigma/r)^{12} - (\sigma/r)^{6}\right]$	ε [kcal mol^{-1}]	$2^{1/6}\sigma/2$ [Å]	m [u]
N	−0.170	1.824	14.010
C0	−0.086	1.908	12.000
C00	−0.708	1.950	12.000
C1	−0.708	1.950	13.008
C2	−0.0705	2.035	14.016
C3	−0.1050	2.050	15.024
C (CNS)	−0.0700	1.9924	12.000

Table 3. Charge distribution on 5CB molecule (charges are given in electrostatic units), taken from [37] (see supporting information)

Site	Charge $\lvert e\rvert$
N	−0.559
C_1	0.767
C_2	−0.804
C_3 (CH), C_4 (CH)	0.242
C_5 (CH), C_6 (CH)	0.156
C_7	−0.211
C_8	−0.330
C_9 (CH), C_{10} (CH)	0.150
C_{11} (CH), C_{12} (CH)	0.196
C_{13}	−0.640
C_{14} (CH_2)	0.286
C_{15} (CH_2)	0.030
C_{16} (CH_2)	−0.056
C_{17} (CH_2)	0.030
C_{18} (CH_3)	−0.004

One way to get a value of diffusion coefficient is integrating the VACF like below:

$$D = \frac{1}{3}\int_0^\infty \langle \vec{v}_i(t)\cdot\vec{v}_i(0)\rangle dt \tag{23}$$

where $\vec{v}_i(t)$ is the centre of mass velocity of a single molecule. The Einstein relation, valid at long times, is another way to compute D

$$2Dt = \frac{1}{3}\langle|\vec{r}_i(t) - \vec{r}_i(0)|^2\rangle \tag{24}$$

$$\langle|\Delta r(t)^2|\rangle \simeq 6Dt \tag{25}$$

where $\vec{r}_i(t)$ is the molecule position.

2.3.2. Structural properties

A second class of observables are the functions that characterize the local structure of a nanomaterial. Most notable among these is the so-called radial distribution function $g(r)$ (RDF). This function gives the probability of finding a pair of atoms at distance r apart, relative to the probability expected for a completely random distribution at the same density [39]. RDF (pair correlation function) describes how the density varies as a function of the distance from a reference particle.

In this dissertation the structure of liquid crystal layers was examined by the radial distribution function:

$$g(r) = \int_{r}^{r+dr} 4\pi\xi^2 p(\xi) d\xi \tag{26}$$

calculated as a histogram of probabilities $p(\xi)$ of finding other molecules in the sphere of the radius between $r+dr$.

As we well know (discussion in chapter 1.1.4) the characterization of a liquid crystalline phase inevitably deals with the investigation of its orientational order, and more generally, with the anisotropy of its physical properties. In case of a rigid molecule this is determined by a non-isotropic distribution of molecular orientations $f(\alpha,\beta,\gamma)$. If we take a director frame as a laboratory frame, the distribution becomes independent of the Euler angle α [40], and if we assume molecular uniaxiality, also from γ, that is, $f = f(\beta)$. the necessary step to calculate $f(\beta)$ is to determine the director at each successive time frame t considered in the MD trajectory [41], and this can be done by setting up and diagonalizing an ordering matrix, Q, given by following equation:

$$Q(t) = \sum_{l=1}^{N} \left[3u_l(t) \otimes u_l(t) - I\right]/2N \tag{27}$$

where $u_l(t)$ is the chosen molecular reference axis, I is the identity matrix and the sum runs over all the N molecules of the sample. The instantaneous order parameter $P_2(t)$ can be obtained from the eigenvalues $\lambda_{\min} < \lambda_0 < \lambda_{\max}$ of the Cartesian ordering matrix $Q(t)$ and this is a suitable observable for describing the nematic–isotropic phase transition. The typical method is using the largest eigenvalue and identify it as the order parameter: $P_2(t) = \lambda_{\max}(t)$. This is a strictly non-negative value, since $Q(t)$ is traceless, so to avoid unrealistically high values of the order parameter in the isotropic phase, $P_2(t)$ is preferably calculated as $P_2(t) = -2\lambda_0(t)$ [42]. The momentary eigenvalues of the ordering matrix can be averaged over a sufficiently long and equilibrated trajectory (indicated by angular brackets), to give the uniaxial order parameter:

$$\langle P_2 \rangle = \langle P_2(t) \rangle = \langle -2\lambda_0(t) \rangle \tag{28}$$

Another way of averaging uses the eigenvectors of $Q(t)$ that provide the instantaneous director frame for the configuration at time t for calculating the Euler angle β between the phase director and the reference axis of molecule i.

This allows computing the overall average of any function of β, and in particular of the second rank Legendre polynomial [37], yielding the corresponding order parameter given by the formula:

$$\langle P_2 \rangle = \left\langle \frac{1}{N} \sum_{i=1}^{n} (3\cos^2\beta - 1)/2 \right\rangle \tag{29}$$

We have decided to chose the eigenvector of the molecule inertia tensor that corresponds to the highest symmetry, as the molecular reference axis. It has been shown in [43] that the order parameter calculated using the inertia axis is slightly higher than in case of choosing the CN bond as a reference axis.

During research we performed many computer simulations of nanosystems. We have decided to present the results which seem to be the most interesting and give theoretical fundamentals for further development. Every investigated ensemble contains a liquid crystal cluster consisting of 5CB molecules (22–98 molecules), often located near the carbon nanostructure (nanotube, graphene). The size of the sample depends on the carbon nanostructure type used in the MD simulation. The molecular structure and modeling has been described in previous sections and a description of the computer simulation details is given below.

Classical equations of motion were integrated using the Brunger-Brooks-Karplus (BBK) method [44] implemented in NAMD [45], with the time step of integration of equations of motion 1 fs (suitable for 5CB model with UA). Simulations were performed in an NVT ensemble and the temperature was controlled using a Langevin thermostat.

3. Results and discussion

Molecular systems embedded in carbon nanotubes are interesting both from the scientific point of view and also because of their interesting potential applications in energy storage, nanoelectronic devices, chemical biosensors, field emission displays and many others. Properties of molecules confined in carbon nanotubes have been intensively studied experimentally [46–48] and using computer simulation methods [49–53].

The simulated system consisted of 40 4-*n*-pentyl-4'-cyanobiphenyl (5CB) molecules encapsulated inside a single-walled, open-ended carbon nanotube. The SWCNT diameter was chosen to be larger than the mesogen length, to make enough space for rotational motions. The 5CB molecule and the SWCNT were modeled using a flexible model based on the CHARMM 27 force field. Interactions between the nanotube and 5CB mesogens were described by the L-J 12–6 potential with Lorentz-Berthelot mixing rules (details in section 2.2). The molecular structure and dynamics of the 5CB molecules were examined by calculating radial distribution functions, the second rank order parameter and the mean square displacement (parallel and perpendicular to the director). The simulations were performed in an NVT ensemble, for the room temperature ($T = 300\,\mathrm{K}$) and for $T = 325\,\mathrm{K}$. The temperature was controlled by a Langevin thermostat with

dumping coefficient $\gamma = 5.0\,\mathrm{ps}^{-1}$. Before each trajectory production, the system was equilibrated for 1 ns. The trajectory data was collected every 25 time steps.

The radial distribution function $g(r)$ of the mass centre of the 5CB molecule is presented in Figure 11. One can see that the $g(r)$ distribution is characteristic for the cluster structure.

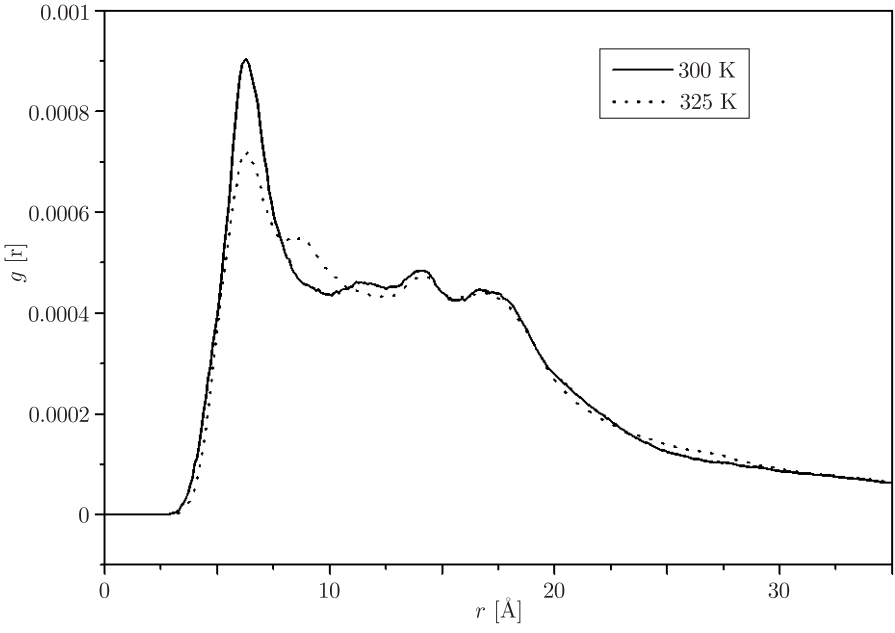

Figure 11. Radial distribution function of 5CB inside the SWCNT at $T = 300\,\mathrm{K}$ and $T = 325\,\mathrm{K}$

The mean square displacement of a mass centre of 5CB molecules for two temperatures is presented in Figure 12. The plots (Figure 13 and Figure 14) of the mean square displacement show a big difference between the mobility of mesogens parallel and perpendicular to the SWCNT surface (the director has the same direction). The diffusion process along the director occurs much faster than the perpendicular diffusion and it is visible for both temperatures. It confirms strong anisotropic properties of the 5CB material encapsulated by the SWCNT. As one can see, the confinement of mesogens induces also a higher molecular order in the cluster ($\langle P_2 \rangle = 0.77$ at $T = 300\,\mathrm{K}$, $\langle P_2 \rangle = 0.76$ at $T = 325\,\mathrm{K}$). The mobility of mesogens increases for the higher temperature but the average order parameter does not decrease. It is an interesting and desired result. Both the anisotropy and spatial orders depend weakly on the temperature, hence the 5CB nematic phase might persist in a wide range of temperatures inside a carbon nanotube.

The studied system is presented in Figure 15. The 40 5CB molecules were embedded in a (20, 20) armchair nanotube of diameter $d = 2.8\,\mathrm{nm}$ and length $\sim 8\,\mathrm{nm}$. The obtained results were then compared with our previous studies of 5CB free clusters and mesogenic systems located between graphene sheets.

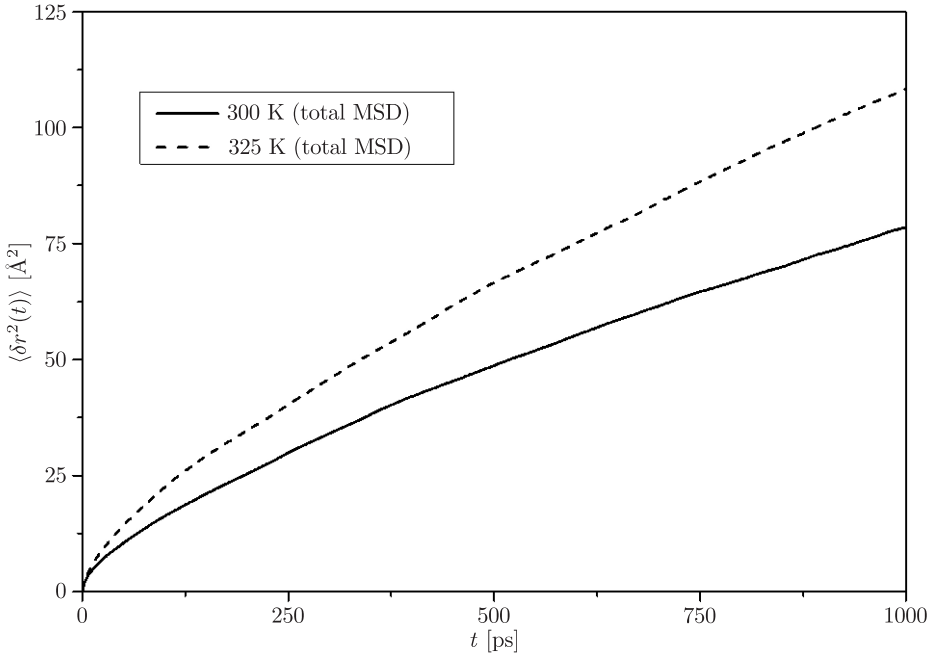

Figure 12. Mean square displacement of centre of mass of 5CB molecule inside carbon nanotube, for two temperatures

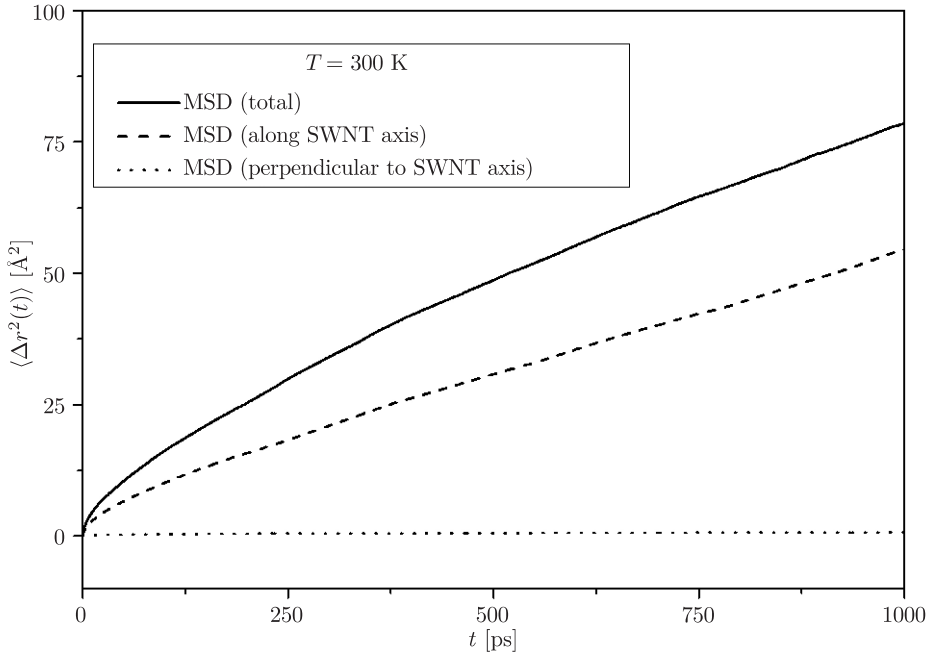

Figure 13. Mean square displacement of centre of mass of 5CB molecule inside carbon nanotube, calculated along different axes (directions)

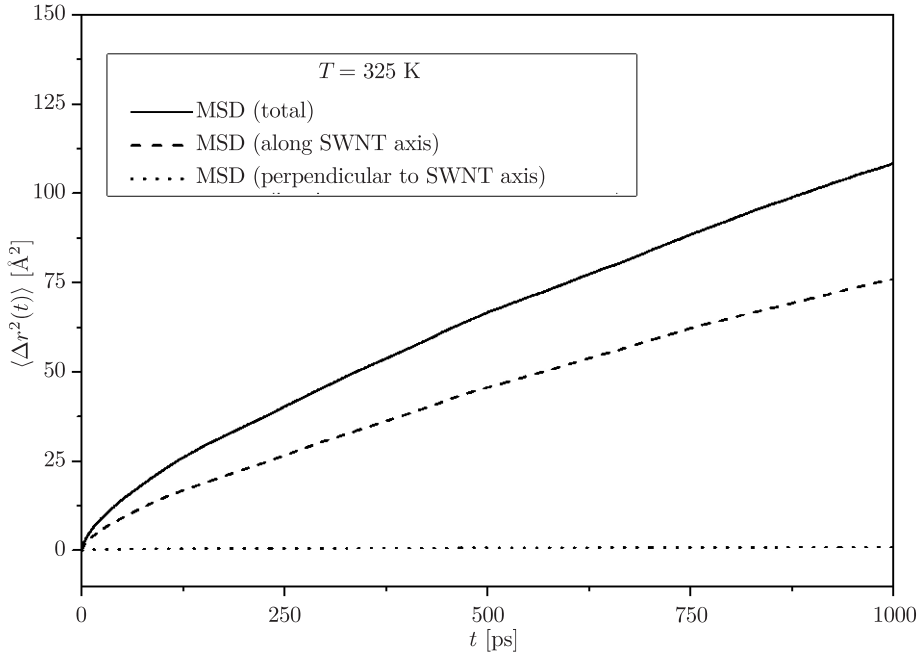

Figure 14. Mean square displacement of the centre of mass of 5CB molecule inside carbon nanotube, at $T = 325\,\mathrm{K}$ calculated along different axes (directions)

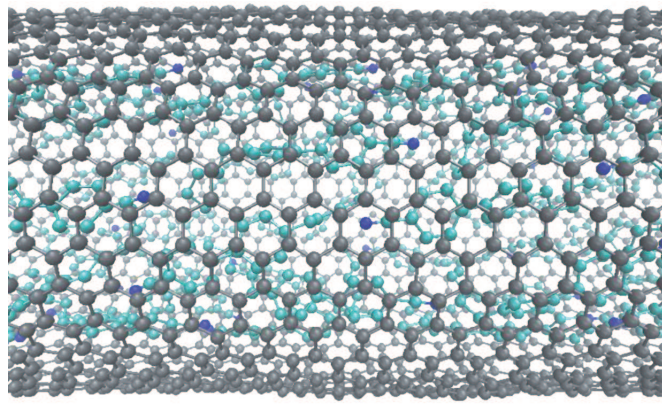

Figure 15. Snapshot of simulated system at $T = 300\,\mathrm{K}$

MD computer experiments were conducted for many physical nanosystems (bulk 5CB sample, a free cluster of 5CB [54], a 5CB layer on a SWCNT [55, 56], a thin layer of 5CB molecules near graphene plane, a 5CB cluster confined in an SWCNT, 5CB mesogens located between two graphene sheets [57]). In all the studied systems with carbon allotropes we observed that the order parameter was higher than in case of free 5 CB clusters or bulk material. As it has been mentioned above the presence of carbon nanostructures stabilizes the nematic phase and it occurs in a wider temperature range. As an example, in Figure 16 we present

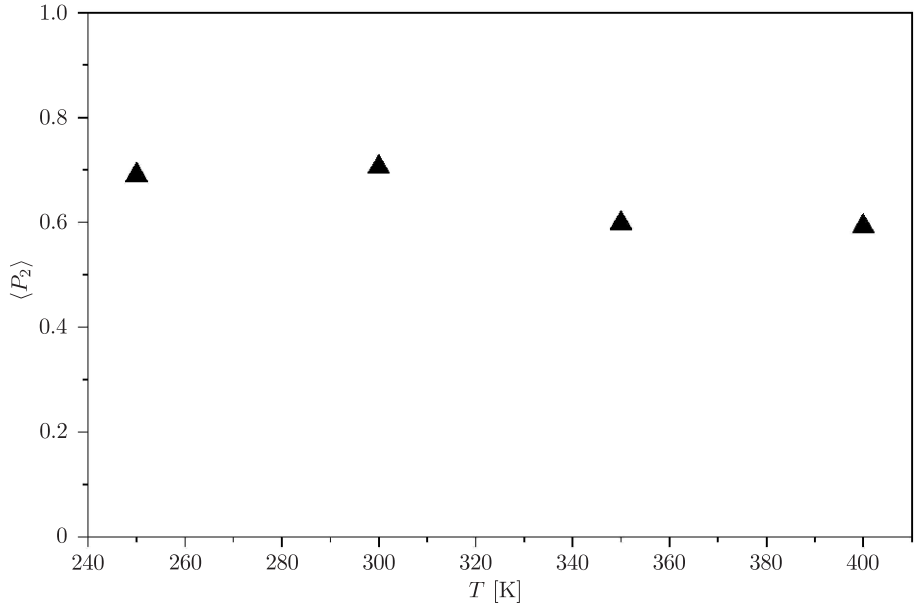

Figure 16. Temperature dependence of second rank order parameter (average value) of $(5CB)_{98}$ between graphene walls

the temperature dependency of the average second rank order parameter for 5CB located between two graphene sheets [57]. These properties of the liquid crystal sample are essential when it comes to technological application. For comparison, the second rank order parameter for the bulk 5CB sample (nematic phase) is $\langle P_2 \rangle^{\text{bulk}} \approx 0.64$ at $T = 300\,\text{K}$ [58]. The nematic–isotropic phase transition for bulk 5CB material appears at $T_{\text{NI}} = 308.5\,\text{K}$ [58] whereas the liquid crystal nematic phase still exists in the simulated mesogenic cluster embedded between graphene walls even at temperature as high as $T = 350\,\text{K}$. The results obtained for 5CB in an SWCNT are even more promising, as the order parameter value is higher than reported in [57].

For all those systems a large number of static and dynamic molecular characteristics of mesogens was presented. However, there is only one observable, order parameter P_2, that can be effectively compared for all those studies.

Table 4 contains data obtained from several different MD simulations and from a real experiment. A computer experiment for the 5CB bulk sample was performed in an NPT ensemble of 196 5CB molecules with periodic boundary conditions. Each other ensemble contained 40 liquid crystal molecules and simulations were performed in an NVT ensemble without periodic boundary conditions.

5CB molecule and carbon structures were modeled using a flexible model based on the CHARMM 27 force field. As one can see Table 4 contains average values of second the rank order parameter and the time evolution of this quantity is shown in Figure 17 for two chosen systems. It is easy to see that placing mesogens near a carbon nanostructure (SWCNT, graphene) increases significantly

Table 4. Average value of second rank order parameter of 5CB mesogens at room temperature in different molecular systems

Ensemble ($T = 300\,\mathrm{K}$)	Second rank order parameter $\langle P_2 \rangle$
$(5CB)_{bulk}$ (experimental data, taken from [58])	0.64
$(5CB)_{196}$ (periodic boundary conditions)	0.51
$(5CB)_{40}$ (free cluster)	0.35
$(5CB)_{40}$ (on SWCNT outer surface)	0.67
$(5CB)_{40}$ (inside SWCNT)	0.77
$(5CB)_{40}$ (on graphene plane)	0.65
$(5CB)_{40}$ (between 2 graphene sheets)	0.71

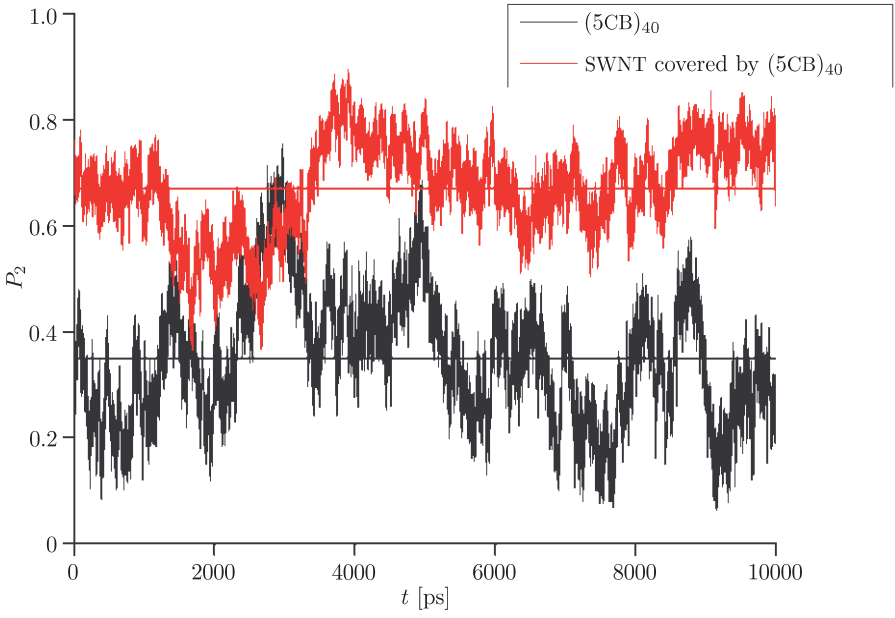

Figure 17. Time evolution of P_2 for two different ensembles at $T = 300\,\mathrm{K}$; solid, horizontal lines correspond to average values of order parameter P_2

the spatial order of the 5CB sample (60 %–100 %). It is worth noting that the largest molecular order is visible in confined systems (5CB inside SWCNT, 5CB between 2 graphene planes). Let us also look at the average value of $\langle P_2 \rangle$ for the bulk material. One can see that $\langle P_2 \rangle^{\mathrm{sim}} < \langle P_2 \rangle^{\mathrm{exp}}$ (20 % less than the experimental data). One of the reasons for such a difference might be the fact that the experimental sample contains much more molecules than the computer modeled ensemble (196 5CB molecules). A typical slab of a nematic for a twisted nematic display has around $2.4 \cdot 10^{11}$ molecules [59]. It should be emphasized that Professor Zannoni's research group obtained a very close result from the MD simulation ($\langle P_2 \rangle \approx 0.51$ at $T = 300\,\mathrm{K}$) [37].

4. Conclusions

In this study we have focused on examining the structural and dynamic properties of $(5CB)_n$ clusters. Under normal circumstances, it appears that a bulk sample of 4-*n*-pentyl-4'-cyanobiphenyl changes dramatically its properties at the temperature of about 310 K. Above this temperature a pure 5CB sample occurs in the isotropic phase and loses the liquid crystalline properties. In this study we have been able to show that placing 5CB molecules near such carbon nanostructures as a nanotube or graphene increases the level of the molecular order. Moreover, the second rank order parameter $\langle P_2 \rangle$ decreases slowly with the increasing temperature. Therefore, the nematic phase of a 5CB cluster may persist in a wider temperature range, which is desirable in certain technical applications. Another important and interesting observation is that embedding 5CB mesogens inside an SWCNT enhances the process of diffusion along the director. The average value of the second rank order parameter is higher than in the 5CB sample adsorbed on the nanotube outer surface.

Some of the presented results seem to be of interest both from the scientific point of view and also due to their potential applications in nanoelectronic devices, chemical biosensors and liquid crystal displays.

References

[1] Gennes P G de and Prost J 2003 *The physics of liquid crystals, 2nd ed.*, Oxford University Press
[2] Collings P J 1990 *Liquid crystals: nature's delicate phase of matter*, Princeton University Press
[3] Singh S 2001 *Liquid Crystals: Fundamentals*, World Scientific Publishing Co. Pte. Ltd.
[4] Fisch M R *Liquid crystals, laptop and life*, *World Scientific Series in Contemporary Chemical Physics* **23**
[5] Kumar S 1995 *Liquid crystals in the nineties and beyond*, World Scientific Publishing Co. Pte. Ltd.
[6] Demus D, Goodby J, Gray G W, Spiess H-W and Vill V 1999 *Physical properties of liquid crystals*, Wiley-VCH
[7] Bilnov L M 2011 *Structures and properties of liquid crystals*, Springer
[8] Zannoni C and Guerra M 1981 *Molec. Phys.* **44** 849
[9] Biscarini F, Chiccoli C, Pasini P and Zannoni C 1991 *Molec. Phys.* **73** 439
[10] Abramowitz M and Stegun I A *Handbook of Mathematical Functions*, Dover Publications
[11] Tsvetkov V 1939 *Acta Physicoch. U.S.S.R.* **10** 557
[12] Luckhurst G R and Veracini C A *The Molecular Dynamics of Liquid Crystals*, Kluwer Academic Publisher
[13] Zannoni C and Pasini P 2000 *Advances in the Computer Simulatons of Liquid Crystals*, Kluwer Academic Publishers
[14] Saito R, Dresselhaus G and Dresselhaus M S 1998 *Physical Properties of Carbon Nanotubes*, Imperial College Press
[15] Singh J 1993 *Physics of Semiconductors and their Heterostructures*, McGraw-Hill
[16] Iijima S 1991 *Nature* **354** 56
[17] Iijima S and Ichihashi T 1993 *Nature* **363** 603

[18] Bethune D S, Kiang C H, Vries M S de, Gorman G, Savoy R, Vazquez J and Beyers R 1993 *Nature* **363** 605
[19] Reich S, Thomsen C and Maultzsch J 2004 *Carbon nanotubes: Basic concepts and physical properties*, Wiley-VCH
[20] Dresselhaus M S, Dresselhaus G and Avouris Ph 2001 *Carbon Nanotubes, Topics in Applied Physics*, Springer
[21] Dresselhaus M S and Avouris Ph 2001 *Topics Appl. Phys.* **80** 1
[22] Kelly B T 1981 *Physics of graphite*, Englewood N J, Applied Science
[23] Savage R H 1948 *Journal of Applied Physics* **19** (1) 1
[24] Dienwiebel M, Verhoeven G S *et al.* *Physical Review Letters* **92** (12) 126101
[25] Zheng Q, Jiang B *et al.* 2008 *Physical Review Letters* **100** (6), 067205
[26] Wallace P R 1947 *Physical Review* **71** (9) 622
[27] Novoselov K S, Geim A K, Morozov S V, Jiang D, Zhang Y, Dubonos S V, Grigorieva I V and Firsov A A 2004 *Science* **306** 666
[28] Frenkel D and Smit B 2002 *Understanding Molecular Simulation: From Algorithms to Applications*, Academic Press
[29] Metropolis N, Rosenbluth A W, Rosenbluth M N, Teller A H and Teller E 1953 *J. Chem. Phys.* **21** 1087
[30] Allen M P and Tildesley D J 1989 *Computer Simulation of Liquids*, Oxford University Press
[31] Rapaport D C *The Art of Molecular Dynamics Simulation*, Cambridge University Press
[32] Hinchliffe A 2003 *Molecular Modelling for Beginners*, John Wiley and Sons
[33] MacDowell L G and Vega C 1998 *J. Chem. Phys.* **109** 5681
[34] Komolkin A V, Laaksonen A and Maliniak A 1994 *J. Chem. Phys.* **101** 4103
[35] Fukunaga H, Takimoto J and Doi M 2004 *J. Chem. Phys.* **120** 7792
[36] Wilson M R 2007 *Chem Soc Rev.* **36** (12) 1881
[37] Tiberio G, Muccioli L, Berardi R and Zannoni C 2009 *Chemphyschem* **10** (1) 125
[38] MacKerell A D Jr, Feig M and Brooks C L III 2004 *J. Comp. Chem.* **25** 1400 Feller S, MacKerell A D Jr 2000 *J. Phys. Chem. B* **104** 7510
[39] 1986 *Molecular-Dynamics Simulation of Statistical-Mechanical Systems*, Ciccotti G and Hoover W G (ed.?)
[40] Rose M E 1957 *Elementary Theory of Angular Momentum*, Wiley
[41] Zannoni C 1979 *The Molecular Physics of Liquid Crystals*, Luckhurst G R and Gray G W (eds.), Academic Press 191
[42] Eppenga R and Frenkel D 1984 *Mol. Phys.* **52** 1303
[43] Pelaez J and Wilson R M 2007 *Phys. Chem. Chem. Phys.* **9** 2968
[44] Brunger A, Brooks C L and Karplus M 1984 *Chem. Phys. Lett.* **105** 495
[45] Phillips J C, Braun R, Wang W, Gumbart J, Tajkhorshid E, Villa E, Chipot C, Skeel R D, Kale L and Schulten K 2005 *J. Comput. Chem.* **26** 1781
[46] Kolesnikov A I, Zanotti J M, Loong C K, Thiyagarajan P, Moravsky A P, Loutfy R O and Burnham C J 2004 *Phys. Rev. Lett.* **93** 35503
[47] Rossi M P, Ye H, Gogotsi Y, Babu S, Ndungu P and Bradley J C 2004 *Nano Lett.* **4** 291
[48] Kim B M, Sinha S and Bau H H 2004 *Nano Lett.* **4** 2203
[49] Marti J and Gordillo M C 2002 *J. Chem. Phys.* **114** 10486
[50] Dendzik Z, Górny K and Gburski Z 2009 *J. Phys. Condens. Matter* **21** 425101
[51] Lin Y, Shiomi J, Maruyama S and Amberg G 2009 *Phys. Rev. B* **80**, 045419
[52] Kofinger J and Dellago C 2009 *Phys. Rev. Lett.* **103**, 080601
[53] Garberoglio G 2010 *Eur. Phys. J. E* **31** 73
[54] Gwizdała W, Dawid A and Gburski Z 2008 *Solid State Phenomena* **140** 89
[55] Gwizdała W, Górny K and Gburski Z 2008 *J. Mol. Struct.* **887** 148

[56] Dawid A and Gwizdała W 2009 *J. Non-Crystalline Solids* **355** 1302
[57] Gwizdała W, Górny K and Gburski Z 2011 *Spectrochimica acta. Part A, Molecular and biomolecular spectroscopy* **79** (4) 701
[58] Vecchi I, Arcioni A, Bacchiocchi C, Tiberio G, Zanirato P and Zannoni C 2007 *Mol. Cryst. Liq. Cryst.* **465** 271
[59] Wilson M R 2005 *Int. Rev. Phys. Chem.* **24** 421